

## Surface enhanced Raman scattering of nanoporous gold: Smaller pore sizes stronger enhancements

L. H. Qian, X. Q. Yan, T. Fujita, A. Inoue, and M. W. Chen<sup>a)</sup>

*International Frontier Center for Advanced Materials, Institute for Materials Research, Tohoku University, Sendai 980-8577, Japan*

(Received 30 January 2007; accepted 12 March 2007; published online 12 April 2007)

The authors report the surface enhanced Raman scattering (SERS) of nanoporous gold with nanopore sizes ranging from 5 to 700 nm. Their comprehensive investigations prove that the strongest SERS enhancement of nanoporous gold takes place from the samples with an ultrafine nanopore size of  $\sim 5$ –10 nm. Both the enhancement factor and detection limit of the ultrafine nanoporous substrate are one to two orders of magnitude better than those of coarsened nonporous gold with smooth surfaces. Moreover, careful microstructure characterization reveals that the anomalous SERS enhancement of the annealed nanoporous gold arises from rough surfaces with characteristic surface irregularities. © 2007 American Institute of Physics.

[DOI: 10.1063/1.2722199]

Surface enhanced Raman scattering (SERS) originates from the improved inelastic scattering of the molecules adsorbed on nanostructured metals and alloys.<sup>1,2</sup> The SERS enhancements generally depend on the nanoscale characteristics of the metallic substrates, such as surface morphology,<sup>3,4</sup> and size and aggregated state of nanoparticles.<sup>5,6</sup> Although extremely high SERS enhancements with single molecule detection have been achieved at “hot spots” where intense electromagnetic fields are believed to generate at interparticle crevices,<sup>7–9</sup> reliable SERS substrates with uniformly ultrahigh SERS enhancements remain to be developed for the practical applications of the SERS effect. A number of attempts have been made to fabricate high-performance SERS substrates, for examples, engraving periodical nanosphere arrays by lithography,<sup>10</sup> self-organizations of nanoparticles in the solutions,<sup>11</sup> and nanoporous substrates.<sup>12–14</sup> Amongst them, nanoporous gold with excellent thermal stability and chemical inactivity has recently been exploited as an attractive substrate for SERS applications because of its large surface area and bicontinuous porous structure in three dimensions.<sup>15</sup> Nevertheless, conventional nanoporous gold with a pore size of about tens of nanometers made by room-temperature dealloying does not show a promising SERS enhancement although nanostructured gold, such as gold nanoparticles, are known to be SERS active for a number of organic and biological molecules.<sup>16</sup> Thus, optimizing the microstructure is crucial to the improvement of the SERS enhancements and thereby the SERS application of nanoporous gold, which has been made an effort by a few of research groups.<sup>17–19</sup> More recently, Kucheyev *et al.* reported that the optimized SERS enhancement can be achieved in the annealed nanoporous gold with a coarsened pore size of  $\sim 250$  nm.<sup>18</sup> However, we found that the strongest SERS enhancement takes place from the nanoporous gold with an ultrafine nanopore size of  $\sim 5$ –10 nm. In this letter we report comprehensive investigations on the SERS effect of nanoporous gold with pore sizes varying from 5 to 700 nm. We prove that the nanoporous gold with a smaller pore size has

stronger SERS enhancements and the anomalous enhancement of the annealed nanoporous gold, observed by Kucheyev *et al.*,<sup>18</sup> is most likely associated with rough gold surfaces caused by contaminations rather than the nanopore size effect.

Two classes of Ag<sub>35</sub>Au<sub>65</sub> (at. %, 50/50 by weight) films with the thicknesses of  $\sim 100$  nm and  $\sim 60$   $\mu\text{m}$ , respectively, were used to synthesize nanoporous gold by selective chemical and electrochemical dealloying in 70% HNO<sub>3</sub> aqueous solution at the temperatures of  $-20$ ,  $0$ , and  $25$  °C, respectively. By controlling the dealloying time and temperatures, we have proven that the nanopore sizes can be tailored from  $\sim 5$  to  $\sim 33$  nm for 100 nm thick films.<sup>19</sup> The 60  $\mu\text{m}$  thick nanoporous gold with a pore size of  $\sim 55$  nm, produced by room-temperature dealloying for 48 h, was further annealed at 200, 300, 400, 500, and 600 °C for 2 h in air, which results in the coarsening of nanoporous gold with pore sizes ranging from 90 to 700 nm. The nanoporous gold specimens with various nanopore sizes were subjected to SERS experiments with rhodamine 6G (R6G) and crystal violet (CV) 10 B as the test molecules. The commercially pure reagents were dissolved into pure water (18.2 M $\Omega$  cm) and methanol, respectively, and the Raman scattering of R6G/nanoporous gold and CV/nanoporous gold was detected by a Ranishaw Raman microscope with 514.5 and 632.8 nm lasers.<sup>20</sup>

Representative micrographs of the nanoporous gold specimens with different pore sizes are illustrated in Figs. 1(a)–1(f). Visible microstructure coarsening during high temperature annealing starts from 200 °C. Thereafter, the porous sizes monotonously increase with annealing temperatures from  $\sim 90$  nm at 200 °C to  $\sim 700$  nm at 600 °C [Fig. 1(f)]. In the annealed samples, the nanoporous structure is still retained, as shown in Fig. 1. It is worthy to note that the surface roughness of gold ligaments strongly depends on the annealing temperatures and surface contaminations. Rough ligament surfaces with more or less characteristic surface irregularities (pimples) always appear as the samples are annealed at a temperature between 400 and 600 °C, accompanying with the coarsening of nanopores and gold ligaments. This surface roughening appears to be related to a pinning effect in the surface diffusion of gold atoms at the medium

<sup>a)</sup> Author to whom correspondence should be addressed; electronic mail: mwchen@imr.tohoku.ac.jp

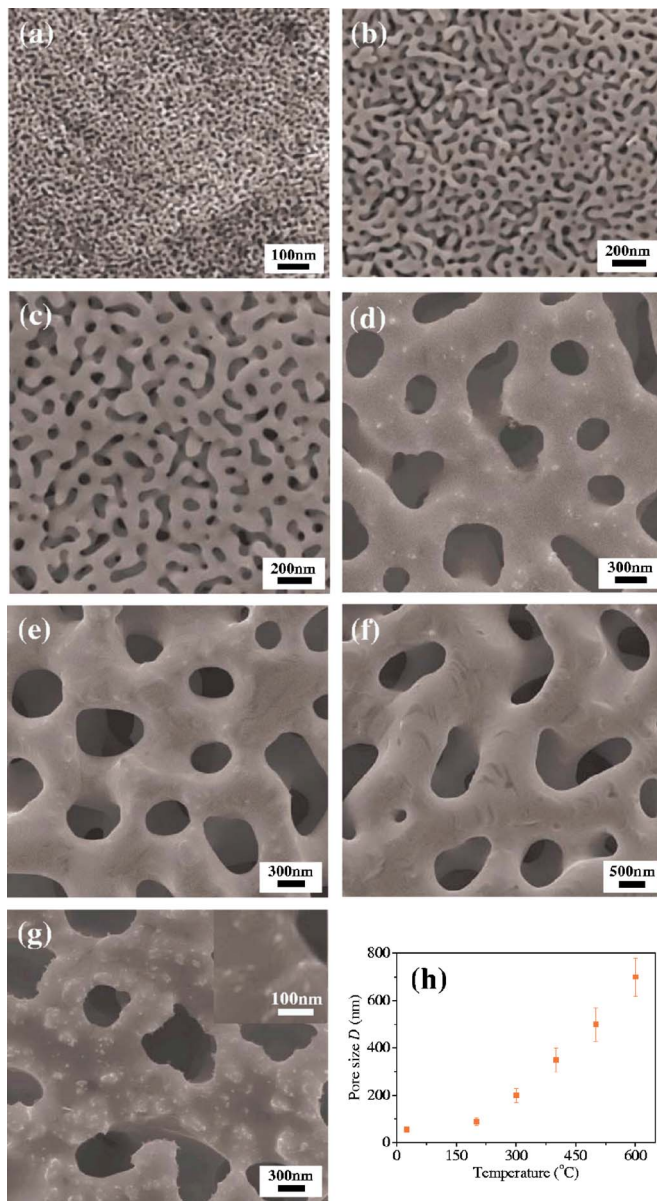


FIG. 1. (Color online) Representative SEM micrographs of nanoporous gold with various nanopore sizes. (a) Nanoporous gold film after 5 min dealloying at room temperature; (b) dealloyed at room temperature for 48 h; (c) thoroughly rinsed nanoporous gold annealed at 200 °C for 2 h; (d) 400 °C for 2 h; (e) 500 °C for 2 h, and (f) 600 °C for 2 h. (g) Nanoporous gold with short-time rinsing and annealed at 600 °C for 2 h. (h) The relationship between nanopore sizes ( $D$ ) of thoroughly rinsed nanoporous gold and the annealing temperatures.

temperatures, caused by the residual acid and silver nitrate on the nanoporous surfaces.<sup>21</sup> We have found that thoroughly rinsing with distilled water for 20 times can dramatically reduce the number of surface irregularities. In contrast, short-time rinsing for only three times lead to the formation of a serious heterogeneous morphology with a large number of “pimples” and relatively small pore sizes after annealing at a temperature between 400 and 600 °C [for example, Fig. 1(g)].

Figure 2(a) illustrates the SERS spectra of R6G molecules on nanoporous gold with various pore sizes. For the as-dealloyed and low temperature annealed nanoporous gold (<300 °C), the nanopores and gold ligaments are much smaller than the laser beam spot ( $\sim 2 \mu\text{m}$  in diameter) and the reproducible spectra can be uniformly attained from dif-

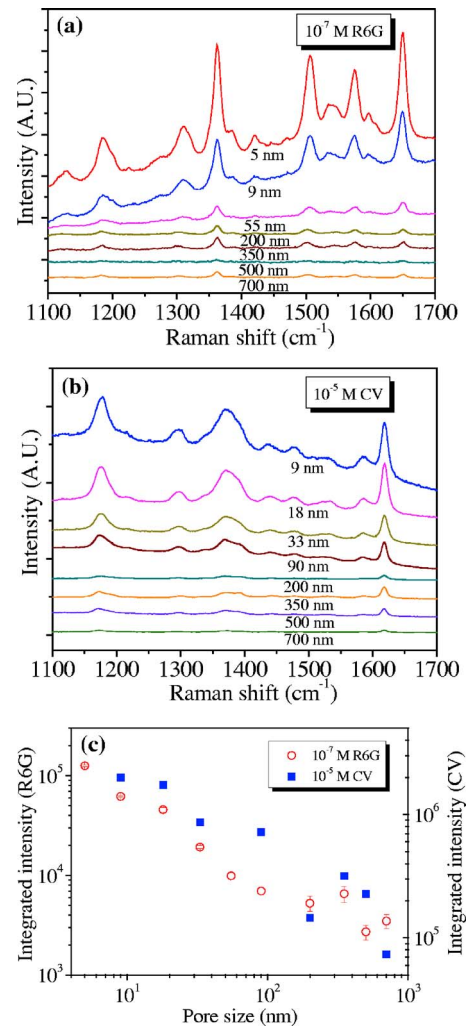


FIG. 2. (Color online) SERS spectra of nanoporous gold with different pore sizes for (a)  $10^{-7}$  mol/l R6G aqueous solution and (b)  $10^{-5}$  mol/l CV methanol solution. (c) Pore size dependence of the integrated intensities of the 1650  $\text{cm}^{-1}$  Raman band at the concentrations of  $1 \times 10^{-7}$  mol/l R6G and 1175  $\text{cm}^{-1}$  Raman band at the concentrations of  $1 \times 10^{-5}$  mol/l CV. Laser excitation: 514.5 nm for R6G and 632.8 nm for CV.

ferent regions of each sample with the same acquisition parameters. However, for the coarsened samples annealed at the temperatures above 300 °C, the intensities of spectra collected from different regions of a sample are inconsistent with 5%–10% variation due to the coarsened nanopores and gold ligaments. Thus, in this study the spectra [Fig. 2(a)] are the average ones acquired from about 10–15 different spots of each sample to show the representative enhancements of nanoporous gold with various pore sizes. Our results prove that the SERS enhancements of nanoporous gold with smooth ligament surfaces are remarkably improved with the reduction of nanopore sizes. The strongest SERS enhancement of nanoporous gold is achieved from a sample with ultrafine pore size of  $\sim 5$  nm. The integrated intensity of R6G 1650  $\text{cm}^{-1}$  Raman band from 5 nm porous gold is more than 24 times stronger than that from 200 nm porous gold annealed at 300 °C [Fig. 2(b)]. Thus, the detection limit of the 5 nm sample approaches to  $5 \times 10^{-10}$  mol/l, which is about one to two orders of magnitude better than that of the annealed samples with smooth gold surfaces. In this study, we do observe the anomalous enhancements from annealed nanoporous gold with a large pore size [Figs. 2(a) and 2(c)],

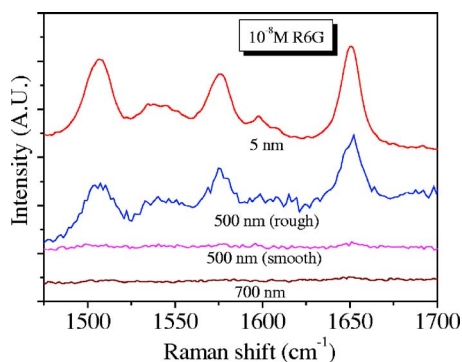


FIG. 3. (Color online) SERS spectra of nanoporous gold with different ligament surface roughness for  $10^{-8}$  mol/l R6G aqueous solution. The spectra collected from 5 and 700 nm nanoporous gold are plotted for comparison.

similar to the observations of Kucheyev *et al.* However, careful microstructure characterization reveals that the anomalous enhancements from the samples with large pore sizes are associated with the rough surfaces of gold ligaments. Figure 3 illustrates the representative SERS spectra of  $10^{-8}$  mol/l R6G solution from the annealed nanoporous gold with different surface roughnesses, as shown in Figs. 1(e) and 1(g). The Raman intensity of the porous sample with a smooth gold surface is almost 15 times weaker than that of 500 nm nonporous gold with a large number of surface irregularities. Apparently, this huge difference in the SERS enhancements cannot be attributed to the minor discrepancy in pore sizes, and most likely results from the difference in the gold surface roughness. Scanning electron microscopy (SEM) characterization reveals that the diameter of the pimples on the rough surfaces is of  $\sim 5\text{--}20$  nm. Interestingly, the SERS enhancement from the regions with a high density of surface pimple is comparable with that from the ultrafine nanoporous gold that possesses an equivalent size in the nanopore diameter as that of the surface irregularities.

To further investigate the optimized SERS enhancements of nanoporous gold, in addition to R6G CV, 10 B in methanol was also used as the test molecules. Figure 2(b) represents SERS spectra of  $10^{-5}$  mol/l CV on nanoporous gold with various pore sizes. Characteristic CV SERS bands can be identified and their intensities gradually increase with the reduction of nanopore sizes. Quantitative intensity measurements of Raman bands at  $1175\text{ cm}^{-1}$  [Fig. 2(c)] show the same size effect as that of R6G, i.e., smaller pore sizes have stronger SERS enhancements. The anomalous enhancement from coarsened nanopores with an  $\sim 350$  nm pore size but a rough gold surface was also evidenced in the CV/nanoporous gold system, as shown in Figs. 2(b) and 2(c). This anomalous enhancement was found to quickly degrade with the smoothing of gold ligament surfaces.

SERS enhancements of nanoporous gold for both R6G and CV molecules prove that ultrafine nanopores possess the strongest SERS enhancement. Although high enhancements can be obtained in the annealed samples with a large pore size of  $\sim 350$  nm, similar to the observations of Kucheyev *et al.*, this anomalous enhancement originates from the ultrafine pimple-type irregularities on the rough gold surfaces. SEM characterization reveals that the diameter of the surface irregularities is of  $\sim 5\text{--}20$  nm. Interestingly, the SERS en-

hancement from the rough ligament surfaces is analogous to that of the ultrafine nanoporous gold with smooth ligament surfaces (Fig. 3). Thus, our observations of the SERS enhancements of nanoporous gold confirm that the high SERS enhancements result from smaller microstructure features, either smaller pore sizes or the rough gold ligament surfaces, which are believed to promote electromagnetic field enhancements and provide more active sites for molecule adsorption.<sup>22,23</sup>

Because the formation and coarsening of nanoporous gold are controlled by surface diffusion, the smaller pore sizes formed by a short dealloying time at low temperatures generally contain more or less residual silver. It is known that the SERS effect of silver exceeds that of gold.<sup>24</sup> Thus, the stronger Raman scattering from the ultrafine nanoporous gold may also include the extra contribution from the residual silver. However, the fact that the annealed nanoporous gold (without detectable residual silver) containing a high density of surface irregularities exhibits the analogous enhancement as the ultrafine nanoporous gold indicates that the ultrafine structures, both small pore sizes and fine surface pimple-type irregularities, play the major role in the strong SERS enhancement of the nanoporous gold.

Research was sponsored by the Grant-in-Aid for Exploratory Research, the Ministry of Education, Culture, Sports, Science and Technology (MEXT), Japan, and by Mitsubishi Science Foundation.

- <sup>1</sup>M. Moskovits, *Rev. Mod. Phys.* **57**, 783 (1985).
- <sup>2</sup>A. Campion and P. Kambhampati, *Chem. Soc. Rev.* **27**, 241 (1998).
- <sup>3</sup>S. Link and M. A. El-sayed, *Int. Rev. Phys. Chem.* **19**, 409 (2000).
- <sup>4</sup>Y. C. Liu, C. C. Yu, and S. F. Sheu, *J. Mater. Chem.* **16**, 3546 (2006).
- <sup>5</sup>P. Hildebrandt and M. Stockburger, *J. Phys. Chem.* **88**, 5935 (1984).
- <sup>6</sup>U. Kreibitz and L. Genzel, *Surf. Sci.* **156**, 678 (1985).
- <sup>7</sup>S. M. Nie and S. R. Emery, *Science* **275**, 1102 (1997).
- <sup>8</sup>K. Kneipp, Y. Wang, H. Kneipp, L. T. Perelman, I. Itzkan, R. R. Dasari, and M. S. Feld, *Phys. Rev. Lett.* **78**, 1667 (1997).
- <sup>9</sup>H. Xu, E. J. Bjerneld, M. Kall, and L. Borjesson, *Phys. Rev. Lett.* **83**, 4357 (1999).
- <sup>10</sup>X. Y. Zhang, A. V. Whitney, J. Zhao, and R. P. Van Duyne, *J. Nanosci. Nanotechnol.* **6**, 1 (2006).
- <sup>11</sup>P. M. Tessier, O. D. Velev, A. T. Kalambur, J. F. Rabolt, A. M. Lenhoff, and E. W. Kaler, *J. Am. Chem. Soc.* **122**, 9554 (2000).
- <sup>12</sup>L. H. Lu, R. Capek, A. Kornowski, N. Gaponik, and A. Eychmuller, *Angew. Chem.* **117**, 6151 (2005).
- <sup>13</sup>Y. Ding, A. Mathur, M. W. Chen, and J. Erlebacher, *Angew. Chem., Int. Ed.* **44**, 4002 (2005).
- <sup>14</sup>Y. Ding, Y. J. Kim, and J. Erlebacher, *Adv. Mater. (Weinheim, Ger.)* **16**, 1897 (2004).
- <sup>15</sup>T. Fujita, L. H. Qian, K. Inoke, J. Erlebacher, and M. W. Chen, *Phys. Rev. Lett.* (in press).
- <sup>16</sup>K. Kneipp, A. S. Haka, H. Kneipp, K. Badizadegan, N. Yoshizawa, C. Boone, K. E. Shafer-peltier, J. T. Motz, R. R. Dasari, and M. S. Feld, *Appl. Spectrosc.* **56**, 150 (2002).
- <sup>17</sup>M. C. Dixon, Ph.D. thesis, Pennsylvania State University, 2005.
- <sup>18</sup>S. O. Kucheyev, J. R. Hayes, J. Biener, T. Huser, C. E. Talley, and A. V. Hamza, *Appl. Phys. Lett.* **89**, 53102 (2006).
- <sup>19</sup>L. H. Qian, X. Q. Yan, T. Fujita, and M. W. Chen (unpublished).
- <sup>20</sup>X. Q. Yan, W. J. Li, T. Goto, and M. W. Chen, *Appl. Phys. Lett.* **88**, 131905 (2006).
- <sup>21</sup>J. Erlebacher, (private communication).
- <sup>22</sup>J. Gersten and A. Nitzan, *J. Chem. Phys.* **73**, 3023 (1980).
- <sup>23</sup>T. Jensen, L. Kelly, A. Lazarides, and G. C. Schatz, *J. Cluster Sci.* **10**, 295 (1999).
- <sup>24</sup>K. Kneipp, M. Moskovits, and H. Kneipp, *Surface-Enhanced Raman Scattering: Physics and Applications* (Springer, Berlin, 2006), 103, p. 261